

Efficient separation of quantum from classical correlations for mixed states with a fixed charge

Christian Carisch¹ and Oded Zilberberg²

¹Institute for Theoretical Physics, ETH Zürich, CH-8093 Zürich, Switzerland.

²Department of Physics, University of Konstanz, 78464 Konstanz, Germany.

Entanglement is the key resource for quantum technologies and is at the root of exciting many-body phenomena. However, quantifying the entanglement between two parts of a real-world quantum system is challenging when it interacts with its environment, as the latter mixes cross-boundary classical with quantum correlations. Here, we efficiently quantify quantum correlations in such realistic open systems using the operator space entanglement spectrum of a mixed state. If the system possesses a fixed charge, we show that a subset of the spectral values encode coherence between different cross-boundary charge configurations. The sum over these values, which we call “configuration coherence”, can be used as a quantifier for cross-boundary coherence. Crucially, we prove that for purity non-increasing maps, e.g., Lindblad-type evolutions with Hermitian jump operators, the configuration coherence is an entanglement measure. Moreover, it can be efficiently computed using a tensor network representation of the state’s density matrix. We showcase the configuration coherence for spinless particles moving on a chain in presence of dephasing. Our approach can quantify coherence and entanglement in a broad range of systems and motivates efficient entanglement detection.

In quantum mechanics, particles can become far more correlated than classically possible. Such correlations, dubbed entanglement, are a key resource in the present-day quantum revolution. For example, entanglement is harvested in quantum information processing devices [1–4], error-correction schemes [5–9], quantum detectors that break sensitivity limits [10–12], or secure

quantum communication protocols [13–15]. Entanglement can also lead to unique effects such as teleportation [16–19], the formation of strong correlations in many-body systems [20–40], and the high efficiency of light-harvesting processes [41–43].

The premise of quantum mechanics relies on having a wavefunction description for particles moving in a closed system. The wavefunction entails probability amplitudes for the state to be in different locations in the Hilbert space of the system. Commonly, the Hilbert space is very large, and entanglement has become a modern tool for compressing the required information needed to properly describe a quantum state [44, 45]. For example, in tensor network representations of quantum states, the Hilbert space is truncated such that only entangled regions are kept [46–48]. As such, measures for quantifying entanglement (e.g., entanglement entropy [1, 49]) were developed to assess the potential usefulness of quantum resources, as well as to compress their representation.

In reality, however, all quantum systems are open, i.e., they are coupled to an environment and become correlated with it. The direct result of such coupling is that the state of the system can become mixed, i.e., lose its entanglement. This is best described by considering the system’s density matrix, which is kin to a covariance matrix of the state’s probability amplitudes. As the density matrix describes both classical and quantum correlations of mixed states, it is notoriously difficult to distill the amount of entanglement in the system. In fact, it is known to be NP-hard to decide whether a mixed state is entangled or not [50, 51]. Many mixed-state entanglement measures have been developed, e.g., (Rényi) negativity [52–56], squashed entanglement [57], reflected entropy [58], or number entanglement [59]. However, so far none of them can be efficiently

computed for reasonably large many-body systems.

In this work, we investigate the degeneracy structure of the operator space entanglement spectrum (OSES) [60–62] and use it to define a tensor network computable measure of cross-boundary coherence and entanglement. We start by rigorously defining the OSES as the eigenvalues of the so-called \mathcal{C} -matrix [44], and analyse it for pure and mixed states separately.

- I. For pure states, we find that the \mathcal{C} -matrix is diagonal with respect to the state's Schmidt basis. We show that the sum over degenerate OSES values quantifies quantum correlations and is closely related to the negativity.
- II. Moving to mixed states, we rely on a fixed charge symmetry, e.g., fixed particle number. We show that under this added assumption, the \mathcal{C} -matrix is block diagonal. We identify that certain blocks have the same eigenvalues. Interestingly, the resulting degenerate OSES values reflect the coherence between different local charge configurations. Hence, we propose their sum as a convex coherence quantifier, which we call the “configuration coherence”. Furthermore, we prove that for purity non-increasing charge conserving maps, the configuration coherence is an entanglement measure.

Importantly, due to easy access to the OSES in tensor network simulations of mixed states, the configuration coherence can be efficiently calculated for many-body system sizes beyond the reach of existing entanglement measures. Finally, we showcase the configuration coherence by measuring the coherence and entanglement in an open quantum system during Lindblad evolution, thus motivating its broad applicability.

The *entanglement spectrum* (ES) of a pure quantum state $|\psi\rangle$ is defined relative to a bipartition (cut) of the system into two parts A and B [see Fig. 1(a)] as the spectrum of the reduced state $\rho_A = \text{Tr}_B(|\psi\rangle\langle\psi|)$. Concurrently, the Schmidt decomposition of the state relative to this cut is

$$|\psi\rangle = \sum_{i=1}^r \sqrt{\lambda_i} |i, \mu_i\rangle, \quad (1)$$

where $r \geq 1$ is the Schmidt rank, $\sqrt{\lambda_i} \geq 0$ are real-valued Schmidt values, and $|i, \mu_i\rangle = |i\rangle_A \otimes$

$|\mu_i\rangle_B$ with suitable orthonormal sets of states for systems A and B . The ES of a state (1) is given by the squares λ_i of its Schmidt values [63]. The corresponding von Neumann entropy, $\mathcal{S}_{\text{vN}} \equiv -\text{Tr}(\rho_A \log \rho_A) = -\sum_i \lambda_i \log \lambda_i$, serves as an entanglement measure for pure states.

Similarly to the pure case, we can define the OSES of a density matrix ρ relative to a bipartition of the system into two parts A and B . The density matrix can be written relative to this bipartition as

$$\rho = \sum_{\substack{i,j \in A \\ \mu,\nu \in B}} \rho_{i,\mu;j,\nu} |i, \mu\rangle\langle j, \nu|, \quad (2)$$

where $|i, \mu\rangle = |i\rangle_A \otimes |\mu\rangle_B$, and $|i\rangle_A$ and $|\mu\rangle_B$ are basis states of the two parts of the system. The density matrix is Hermitian, and hence the prefactors in Eq. (2) follow the relation $\rho_{i,\mu;j,\nu} = \rho_{j,\nu;i,\mu}^*$. We define the vectorized density matrix as

$$|\rho\rangle \equiv \sum_{\substack{i,j \in A \\ \mu,\nu \in B}} \rho_{i,\mu;j,\nu} |i, \mu; j, \nu\rangle, \quad (3)$$

which is obtained by stacking the columns of the density matrix (2) into a column vector. The inner product over such column vectors in terms of their respective density operators is defined as $\langle\langle\rho|\sigma\rangle\rangle \equiv \text{Tr}(\rho^\dagger \sigma)$. The OSES of ρ consists of the eigenvalues of the matrix [44]

$$\begin{aligned} \mathcal{C} &= \text{Tr}_B(|\rho\rangle\langle\rho|) \\ &= \sum_{\substack{i,j,k,l \in A \\ \mu,\nu \in B}} \rho_{i,\mu;j,\nu} \rho_{k,\mu;l,\nu}^* |i, j\rangle\langle k, l|, \end{aligned} \quad (4)$$

where $\text{Tr}_B \mathcal{O} = \sum_{\mu,\nu \in B} \langle\langle\mu, \nu|\mathcal{O}|\mu, \nu\rangle\rangle$ is the partial trace over subsystem B . The matrix (4) is a positive operator that involves correlations up to fourth order in the state's probability amplitudes, and we dub it the kurtosis matrix. As we show below, the OSES contains values encoding both classical correlations as well as entanglement, raising doubts concerning its naming convention. Interestingly, the sum over both classical and quantum OSES values equals to the purity of the system, i.e., $\text{Tr} \mathcal{C} = \text{Tr}(|\rho\rangle\langle\rho|) = \text{Tr} \rho^2 \equiv \mathcal{P}(\rho)$.

Ostensibly, we would like to employ the operator space entanglement entropy (OSEE), $\mathcal{S} \equiv -\text{Tr}(\mathcal{C} \log \mathcal{C})$, as an entanglement measure. Yet, it appears to be sensitive to both

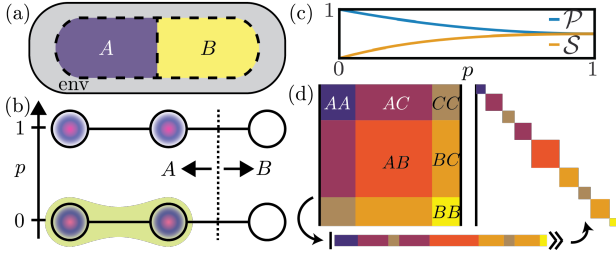


Figure 1: (a) An open bipartite system $A \cup B$ in contact with an environment. (b) A single particle on a 3-site system is distributed over sites 1 and 2 (subsystem A), as a function of mixing [cf. Eq. (5)] from pure ($p = 0$) to fully mixed ($p = 1$). Yellow shading marks quantum correlations, which are lost in the fully mixed limit. (c) Purity \mathcal{P} of the whole system and OSEE \mathcal{S} between A and B in (b) as a function of mixing p . The OSEE increases despite the fact that the mixing does not affect cross-boundary correlations. (d) Pictorial derivation of the block diagonal structure of the \mathcal{C} -matrix [cf. Eq. (9)]. For example, the 2-particle density matrix has entries corresponding to the particles' configurations, e.g., both in subsystem A (AA), or one in A and one in B (AB). When a particle is coherently delocalized across the bipartition, we use C . After vectorizing the density matrix [cf. Eq. (3)], the partial trace reveals the block diagonal structure [cf. Eqs. (4) and (9)].

classical and quantum correlations [61, 64]. The latter is evident from our construction (4) using a counterexample: consider a pure state with a single excitation residing solely within subsystem A , e.g., subsystem A is composed of states $|1\rangle$ and $|2\rangle$, whereas subsystem B of state $|3\rangle$, see Fig. 1(b). We take the quantum state to be in an equal superposition, $|\psi\rangle = (|1\rangle + |2\rangle)/\sqrt{2}$. The corresponding OSES has a single nonvanishing value Λ_A [cf. Eq. (9) and discussion below]. Hence, for our pure system $\Lambda_A = \text{Tr}(\mathcal{C}) = \mathcal{P}(\rho) = 1$. Correspondingly, $\mathcal{S} \equiv -\Lambda_A \log \Lambda_A = 0$ as expected for a pure product state. We now locally couple subsystem A to a dephasing environment, i.e., no particles leak out, but the system decoheres into a mixed state ρ' after some time. As the particle remains in subsystem A , we still have a single eigenvalue Λ'_A that corresponds to a reduced purity $\mathcal{P}(\rho') < 1$ of the system. Thus, we obtain that the OSEE increases to $\mathcal{S}' = -\Lambda'_A \log \Lambda'_A > 0$ even though the local operation on subsystem A cannot have generated entanglement between subsystems A and B . This is a first important observation of this work.

In Fig. 1(c), we show the outcome of our counterexample with increasing dephasing. The latter

is obtained by mixing the pure state with the classical mixture of the particle being either in state $|1\rangle$ or $|2\rangle$, namely by

$$\rho_p = (1-p)|\psi\rangle\langle\psi| + p\sigma, \quad (5)$$

with $\sigma = (|1\rangle\langle 1| + |2\rangle\langle 2|)/2$, see Fig. 1(b). The OSEE increases with increasing weight p of the separable classical mixture, confirming the deficiency of the OSEE as an entanglement measure for mixed states. Crucially, we identify that part of the OSES bears no entanglement information, e.g., Λ_A in our example. Hence, any entanglement measure should filter out such values, which may be challenging for a many-body system on a large Hilbert space.

For pure states $|\psi\rangle$, however, the filtering is relatively straightforward: we can write the \mathcal{C} -matrix (4) of a density matrix $|\psi\rangle\langle\psi|$ using the state's Schmidt basis [cf. Eq. (1)] as

$$\mathcal{C} = \sum_i \lambda_i^2 |i, i\rangle\langle i, i| + \sum_{j \neq i} \lambda_i \lambda_j |i, j\rangle\langle i, j|. \quad (6)$$

In this basis, the \mathcal{C} -matrix is diagonal and its spectrum consists of r eigenvalues of type λ_i^2 and $r(r-1)/2$ two-fold degenerate eigenvalues of type $\lambda_i \lambda_j$. Thus, in this pure limit, the OSES of the density matrix is equivalent to the outer product of the ES of the state [44, 65]. We can also readily verify using Eq. (6) that only a single nonvanishing λ_i^2 value appears in the pure limit of the example of Fig. 1(b).

Now, recall that a pure state (1) is entangled if and only if its Schmidt rank is $r > 1$. As the second sum in Eq. (6) vanishes for $r = 1$ and is finite and positive for $r > 1$, we propose the sum over these eigenvalues as a quantifier of quantum correlations in pure states,

$$C_N(|\psi\rangle) := \sum_{j \neq i} \lambda_i \lambda_j. \quad (7)$$

In other words, we obtain the quantum correlations of a pure state as the sum over inherently degenerate eigenvalues of the matrix \mathcal{C} and filter out the λ_i^2 values.

Interestingly, the quantity (7) is closely related to the negativity of the state, which is defined as the absolute value of the sum over all negative eigenvalues of the partial transpose ρ^{TB} of the density matrix [52]. Indeed, using the Schmidt decomposition (1), the negativity reads

$$\mathcal{N} = \frac{1}{2} \sum_{j \neq i} \sqrt{\lambda_i} \sqrt{\lambda_j}. \quad (8)$$

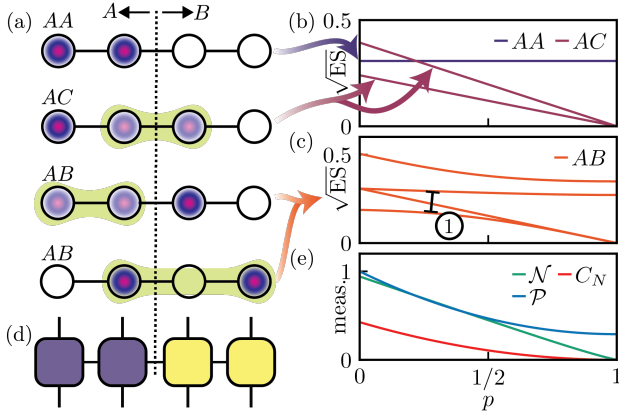


Figure 2: (a) Examples of configurations of two particles on four sites with respect to a bipartition in the middle. Yellow shadings mark quantum correlations. (b) and (c) OSES corresponding to the configurations in (a) along a mixing interpolation [cf. Eq. (5)]. (1) marks an avoided crossing between spectral values of a classically and a quantum correlated AB configuration. (d) MPDO representation of a density matrix on 4 sites. (e) Negativity \mathcal{N} , purity \mathcal{P} , and configuration coherence C_N for the spectrum in (b) and (c).

Thus, our Eq. (7) defines a new way to calculate the negativity for pure states: it is obtained as the sum over the square roots of the degenerate eigenvalues of the \mathcal{C} -matrix. This is a second important observation of this work. Furthermore, the definition of the quantity (7) via the matrix \mathcal{C} lends a natural extension to open systems. The remaining challenge involves the identification of \mathcal{C} -matrix eigenvalues that encode cross-boundary quantum correlations for mixed states.

Before turning to discuss the OSES of mixed states in more detail, we present some general comments about mixed state entanglement. As mentioned above, the mixed state separability problem is NP-hard [50, 51]. The complexity of the problem should therefore be reduced in order to develop a computable mixed state entanglement measure. Here, we impose a symmetry to restrict the relevant Hilbert space dimension. Within this space, we consider states which have a fixed value of the symmetry's conserved charge. Without loss of generality, we study systems with a fixed number of N particles. This restriction leads to degeneracies in the OSES, which allow us to define the configuration coherence as a measure of quantum coherence. We prove that the configuration coherence is an entanglement measure under purity non-increasing charge conserving maps. Our approach is related to recent stud-

ies of symmetry-resolved coherence and entanglement measures [59, 66, 67].

We write the density matrix (2) using the basis states $|i_n, \mu_n\rangle$ with $0 \leq n \leq N$ particles in subsystem B and $N - n$ particles in subsystem A . The \mathcal{C} -matrix in this basis is block diagonal,

$$\mathcal{C} = \bigoplus_{n,n'=0}^N \mathcal{C}_{n,n'}, \quad (9)$$

with blocks

$$\mathcal{C}_{n,n'} = \sum_{i_n, j_{n'}, k_n, l_{n'}} c_{i_n, j_{n'}, k_n, l_{n'}} |i_n, j_{n'}\rangle \langle k_n, l_{n'}| \quad (10)$$

and coefficients

$$c_{i_n, j_{n'}, k_n, l_{n'}} = \sum_{\mu_n, \nu_{n'}} \rho_{i_n, \mu_n; j_{n'}, \nu_{n'}} \rho_{k_n, \mu_n; l_{n'}, \nu_{n'}}^* \quad (11)$$

A graphical derivation of this block diagonal form is shown in Fig. 1(d). Importantly, we can interpret the blocks in terms of configurations of the N particles with respect to the bipartition: the block $\mathcal{C}_{n,n'}$ contains all information on $\min(n, n')$ particles that are fully in subsystem B , $N - \max(n, n')$ particles that are fully in subsystem A , and $\max(n, n') - \min(n, n')$ particles that are coherently distributed across the cut.

In the following, we compare the eigenvalues of the blocks $\mathcal{C}_{n,n'}$ with the pure case limit (6) to distinguish classical from quantum correlations for mixed states. We accompany our discussion with an example of a chain with $N = 2$ spinless particles residing on 4 sites, see Fig. 2. We begin with the blocks $\mathcal{C}_{0,0}$ and $\mathcal{C}_{N,N}$, which are rank 1 and have eigenvalues $\Lambda_{0,0} = \sum_{i,j} |\rho_{i,0;j,0}|^2$ and $\Lambda_{N,N} = \sum_{\mu,\nu} |\rho_{0,\mu;0,\nu}|^2$, corresponding respectively to the scenario where all N particles reside solely in subsystem A or B , see Fig. 2(a). These eigenvalues do not contain any information about cross-boundary coherence nor contribute to quantum correlations between subsystems A and B . Indeed, these values are generally non-degenerate, and we identify that they reduce to eigenvalues of type λ_i^2 in the pure case limit, cf. Eq. (6). Furthermore, such values do not vanish for a fully mixed state [see Fig. 2(b)], justifying our choice to not include them in our correlation measure (7).

The blocks $\mathcal{C}_{n,n'}$ for $n \neq n'$ describe a scenario where at least one of the particles is in a coherent

cross-boundary state and clearly encode cross-boundary coherence. The blocks $\mathcal{C}_{n,n'}$ and $\mathcal{C}_{n',n}$ generate the same eigenvalues as they are related via a unitary transformation, $\mathcal{C}_{n,n'} = U\mathcal{C}_{n',n}U^{-1}$, with the permutation $U|i, j'\rangle = |j', i\rangle$. Hence, such coherent eigenvalues of \mathcal{C} are inherently degenerate, and must map to the eigenvalues of type $\lambda_i\lambda_j$ in the pure case limit (6). Therefore, we employ these eigenvalues to extend the pure state correlation measure (7) to the mixed case. Specifically, we define the *configuration coherence* as their sum,

$$\begin{aligned} C_N(\rho) &:= \sum_{n \neq n'} \text{Tr}(\mathcal{C}_{n,n'}) \\ &= \sum_{n \neq n'} \sum_{\substack{i_n, j_{n'} \\ \mu_n, \nu_{n'}}} |\rho_{i_n, \mu_n; j_{n'}, \nu_{n'}}|^2. \end{aligned} \quad (12)$$

Crucially, the configuration coherence contains only off-diagonal elements of the density matrix, which vanish in the fully decohered case, in conjunction with the fact that the fully decohered state contains no quantum correlations, see Figs. 2(a), (b), and (e). That the configuration coherence can be written in terms of off-diagonal density matrix entries explains our naming choice: quantum coherence is identified with the off-diagonal elements of the density matrix.

Before we turn to discuss the properties of the configuration coherence, let us highlight the key aspects of our derivation of Eq. (12). We started with the \mathcal{C} -matrix (9) of a mixed state with a fixed particle number. In any bipartite basis $|i_n, \mu_n\rangle$, the \mathcal{C} -matrix is block-diagonal and the blocks $\mathcal{C}_{n,n'}$ reflect different local charge configurations (n, n') . Therefore, we can identify their basis-independent eigenvalues (their OSES values) with the charge configurations. We have shown that the blocks $\mathcal{C}_{n,n'}$ and $\mathcal{C}_{n',n}$ for $n \neq n'$ lead to the same eigenvalues and that therefore the OSES is degenerate. Finally, we sum up the degenerate OSES values by summing the traces of the degenerate blocks $\mathcal{C}_{n \neq n'}$ and arrive at the configuration coherence (12). Importantly, we did not impose any further restriction onto the mixed state except for the presence of a fixed charge. Moreover, the configuration coherence (12) is basis independent, which is more apparent in our alternative definitions (17) and (21) in appendix A.

The measure C_N encodes the coherence between sectors of different local particle numbers (n, n') and has the following properties:

1. It vanishes for separable states with fixed particle number.
2. It is convex, i.e., $C_N(\sum_i p_i \rho_i) \leq \sum_i p_i C_N(\rho_i)$ for density matrices ρ_i and $\sum_i p_i = 1$.
3. It is invariant under local particle number conserving unitary operations.
4. It is monotonously decreasing under local purity non-increasing particle number conserving operations.

Proofs for these statements can be found in appendix A. Let us briefly discuss the implications of these properties. Property 1 means that the configuration coherence is an entanglement witness for systems with a fixed particle number: if the state of such a system has non-zero configuration coherence, it cannot be separable, i.e., it is entangled. Due to property 3, the configuration coherence is independent of the local basis choice and cannot be changed by isolated subsystem evolution. Property 4, in combination with the ability to witness entanglement, makes the configuration coherence an entanglement measure under purity non-increasing particle number conserving maps [68]. The most general purity non-increasing maps are unital maps, i.e., those that preserve the completely mixed state [69, 70]. Importantly, these include evolutions governed by a Lindblad master equation with Hermitian jump operators [71], making the configuration coherence a powerful and versatile quantifier for coherence and entanglement. The definition of the configuration coherence (12) together with its properties is the main result of this work.

The remaining blocks of the \mathcal{C} -matrix with $n = n' \notin [0, N]$ describe both classical and quantum correlations. This is evident from their pure limit, where they exhibit both non-degenerate and degenerate eigenvalues, of which only the latter contribute to the measure (7), see Fig. 2(c). Note that when the state is mixed, the degeneracy may be lifted via avoided crossings between classical- and quantum-correlation values (see marker (1) in Fig. 2(c)). In this situation, it is in general not possible to assign the OSES values of such blocks to classical or quantum correlations. We, therefore, do not include these values in the configuration coherence (12). The OSES values of the $n = n' \notin [0, N]$ mix information about classical and quantum correlations within the $n = n'$

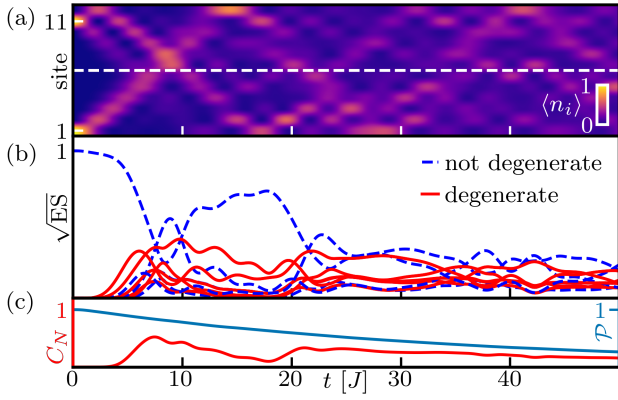


Figure 3: Two particles hopping on a 12-site chain while subject to dephasing [cf. Eq. (14)], implemented in MPDO-TEBD with timestep $dt = 0.05J$, dephasing strength $\gamma = 0.005J$, and maximal bond dimension $\chi = 200$. (a) Local particle densities $\langle n_i \rangle$ as a function of space along time. Dashed white line denotes bipartition at the middle bond. (b) Evolution of the OSES at the bipartition. Blue-dashed lines: non-degenerate OSES values. Red lines: degenerate OSES values encoding the cross-boundary coherence. (c) Configuration coherence C_N and purity \mathcal{P} calculated as the sum over the degenerate and all OSES values, respectively.

charge sector, and the classical correlations would tamper with the desirable properties of the configuration coherence. Specifically, the configuration coherence would neither be an entanglement witness (classically correlated states would have non-zero configuration coherence) nor an entanglement monotone (by increasing classical correlations we could increase the configuration coherence). Distilling the amount of quantum correlations contained in such OSES values will be the topic of future work.

The remaining challenge involves the efficient spectral filtering of a density matrix ρ describing a mixed state of a realistic open quantum system with fixed particle number. For one dimensional systems, we propose to compute the configuration coherence using a matrix product density operator (MPDO) decomposition of ρ [72] [cf. Fig. 2(d)]. The MPDO description gives direct and efficient access to the OSES [48]. In principle, the configuration coherence (12) can then be obtained as the sum over the degenerate values. However, there might be accidental degeneracies due to level crossings in the spectrum, see Fig. 2(b). Such degeneracies can be revealed by a small continuous deformation of the MPDO,

e.g., using an interpolation of the form

$$\rho_p = (1 - p)\rho + p\text{diag}(\rho). \quad (13)$$

This interpolation can be applied independent of the representation of the density matrix, and it is straightforwardly implemented within the MPDO formalism: The diagonal state $\text{diag}(\rho)$ is obtained by setting the off-diagonal elements of the local MPDO-matrices to zero and the addition is an efficient operation for MPDOs (the bond dimension of a sum of MPDOs is bounded by the sum of the individual bond dimensions). It is important to note that the computability of the configuration coherence from an MPDO-representation of a mixed state at no additional computational cost is a major advantage of our approach. In comparison, the calculation of the negativity requires additional diagonalization of an exponentially large operator.

We turn now to showcase the configuration coherence in a realistic open system scenario. We consider a system of $N = 2$ spinless particles moving on a 1D chain with 12 sites in the presence of dephasing. For this system, we can readily obtain an exact MPDO representation because of the small rank of the \mathcal{C} -matrix, see appendix B. For larger systems requiring a truncated MPDO description, our algorithm will yield a tight lower bound on the configuration coherence. The time evolution follows a Lindblad master equation

$$\partial_t \rho = -i[H, \rho] + \gamma \sum_i (2n_i \rho n_i - \{n_i, \rho\}) , \quad (14)$$

with a hopping Hamiltonian

$$H = J \sum_i c_i^\dagger c_{i+1} + h.c. , \quad (15)$$

and local density operators $n_i = c_i^\dagger c_i$. The parameters J and γ are the hopping amplitude and the dephasing coupling rate to local baths, respectively. As discussed above, by property 4 and the unitality of the evolution (14), it follows that the configuration coherence is a faithful entanglement measure for this example.

We initialise the system in a product state of one particle on site 1 and the other on site 11, and evolve Eq. (14) using time evolving block decimation (TEBD) with the JULIA ITensors package [73]. In Fig. 3(a), we present the resulting density of the two particles. The OSES associated with a half-chain bipartition is directly obtained

from the MPDO representation throughout the time evolution, see Fig. 3(b). As expected for a product state, the OSES at $t = 0$ consists of a single value only, describing one particle in each of the subsystems to the left and right of the cut. Along the time evolution, the particles delocalize across the cut, leading to cross-boundary coherence and entanglement, evident by the emergence of degenerate OSES values. We extract the configuration coherence (12) as the sum over the degenerate OSES values and the purity as the sum over all OSES values, see Fig. 3(c). The dissipative Lindblad terms continuously decrease the purity.

In conclusion, we have analyzed the OSES for general pure states as well as mixed states with a fixed particle number. For pure states, the sum over degenerate OSES values lends a quantifier of quantum correlations that is closely related to the negativity. For mixed states with fixed particle number, we defined the sum over degenerate OSES values as the configuration coherence. The configuration coherence is a basis-independent witness of entanglement between sectors with different local particle numbers. Moreover, for purity non-increasing particle number conserving maps such as Lindblad-type evolutions with Hermitian jump operators, the configuration coherence is an entanglement measure. As an example, we have measured the entanglement of spinless particles using a MPDO-TEBD algorithm. Thus, we have shown that the configuration coherence can be efficiently computed for 1D systems with a suitable low-rank MPDO representation. Such systems include infinite size dissipative quantum chains [74], open many-body localized systems [75–77], strongly thermalizing systems [78], exciton dynamics [79], the quantum Heisenberg magnet [80], and temporal entanglement in many-body Floquet dynamics [81, 82]. Experimentally, the configuration coherence can be obtained by estimating the purity of the mixed state [83, 84] and subtracting the values encoding classical correlations; the latter are constructed out of local density measurements. Our results facilitate the study of entanglement and coherence in contemporary noisy intermediate-scale quantum era systems [85, 86] and motivate further OSES-based measures and complexity estimates. A natural extension of our work will involve the potential of discarding the fixed charge assumption

for the mixed state. In a first step, one could calculate perturbative corrections to the degenerate OSES values if a second charge sector weakly contributes to the mixed state. We expect the perturbation to lift the degeneracies. This will also happen when there is no symmetry in the system. In this case, the degeneracy structure of the OSES might contain different information.

Acknowledgments. We thank E. van Nieuwenburg, M. S. Ferguson, A. Štrkalj, M. H. Fischer, L. Stocker, A. Romito, J. del Pino, D. Sutter, J. Renes, M. Michalek, and S. Ryu for fruitful discussions. We thank Z. Ma, C. Han, and E. Sela for pointing out a wrong statement in an earlier version of this manuscript and for drawing our attention to their related work on number entanglement [59]. We acknowledge financial support by ETH Research Grant ETH-51 20-1 and the Deutsche Forschungsgemeinschaft (DFG) - project number 449653034.

References

- [1] Michael A. Nielsen and Isaac L. Chuang. *Quantum Computation and Quantum Information: 10th Anniversary Edition*. Cambridge University Press, 2010. DOI: [10.1017/CBO9780511976667](https://doi.org/10.1017/CBO9780511976667).
- [2] Sergio Boixo, Sergei V. Isakov, Vadim N. Smelyanskiy, Ryan Babbush, Nan Ding, Zhang Jiang, Michael J. Bremner, John M. Martinis, and Hartmut Neven. Characterizing quantum supremacy in near-term devices. *Nature Physics*, 14(66): 595–600, Jun 2018. ISSN 1745-2481. DOI: [10.1038/s41567-018-0124-x](https://doi.org/10.1038/s41567-018-0124-x).
- [3] C. Neill, P. Roushan, K. Kechedzhi, S. Boixo, S. V. Isakov, V. Smelyanskiy, A. Megrant, B. Chiaro, A. Dunsworth, K. Arya, R. Barends, B. Burkett, Y. Chen, Z. Chen, A. Fowler, B. Foxen, M. Giustina, R. Graff, E. Jeffrey, T. Huang, J. Kelly, P. Klimov, E. Lucero, J. Mutus, M. Neeley, C. Quintana, D. Sank, A. Vainsencher, J. Wenner, T. C. White, H. Neven, and J. M. Martinis. A blueprint for demonstrating quantum supremacy with superconducting qubits. *Science*, 360(6385):195–199, Apr 2018. DOI: [10.1126/science.aao4309](https://doi.org/10.1126/science.aao4309).
- [4] Frank Arute, Kunal Arya, Ryan Babbush, Dave Bacon, Joseph C. Bardin, Rami

- Barends, Rupak Biswas, Sergio Boixo, Fernando G. S. L. Brandao, David A. Buell, Brian Burkett, Yu Chen, Zijun Chen, Ben Chiaro, Roberto Collins, William Courtney, Andrew Dunsworth, Edward Farhi, Brooks Foxen, Austin Fowler, Craig Gidney, Marissa Giustina, Rob Graff, Keith Guerin, Steve Habegger, Matthew P. Harrigan, Michael J. Hartmann, Alan Ho, Markus Hoffmann, Trent Huang, Travis S. Humble, Sergei V. Isakov, Evan Jeffrey, Zhang Jiang, Dvir Kafri, Kostyantyn Kechedzhi, Julian Kelly, Paul V. Klimov, Sergey Knysh, Alexander Korotkov, Fedor Kostritsa, David Landhuis, Mike Lindmark, Erik Lucero, Dmitry Lyakh, Salvatore Mandrà, Jarrod R. McClean, Matthew McEwen, Anthony Megrant, Xiao Mi, Kristel Michielsen, Masoud Mohseni, Josh Mutus, Ofer Naaman, Matthew Neeley, Charles Neill, Murphy Yuezhen Niu, Eric Ostby, Andre Petukhov, John C. Platt, Chris Quintana, Eleanor G. Rieffel, Pedram Roushan, Nicholas C. Rubin, Daniel Sank, Kevin J. Satzinger, Vadim Smelyanskiy, Kevin J. Sung, Matthew D. Trevithick, Amit Vainsencher, Benjamin Villalonga, Theodore White, Z. Jamie Yao, Ping Yeh, Adam Zalcman, Hartmut Neven, and John M. Martinis. Quantum supremacy using a programmable superconducting processor. *Nature*, 574(77797779):505–510, Oct 2019. ISSN 1476-4687. DOI: [10.1038/s41586-019-1666-5](https://doi.org/10.1038/s41586-019-1666-5).
- [5] Charles H. Bennett, David P. DiVincenzo, John A. Smolin, and William K. Wootters. Mixed-state entanglement and quantum error correction. *Phys. Rev. A*, 54:3824–3851, Nov 1996. DOI: [10.1103/PhysRevA.54.3824](https://doi.org/10.1103/PhysRevA.54.3824).
- [6] D. G. Cory, M. D. Price, W. Maas, E. Knill, R. Laflamme, W. H. Zurek, T. F. Havel, and S. S. Somaroo. Experimental quantum error correction. *Phys. Rev. Lett.*, 81: 2152–2155, Sep 1998. DOI: [10.1103/PhysRevLett.81.2152](https://doi.org/10.1103/PhysRevLett.81.2152).
- [7] Philipp Schindler, Julio T. Barreiro, Thomas Monz, Volckmar Nebendahl, Daniel Nigg, Michael Chwalla, Markus Hennrich, and Rainer Blatt. Experimental repetitive quantum error correction. *Science*, 332(6033): 1059–1061, May 2011. DOI: [10.1126/science.1203329](https://doi.org/10.1126/science.1203329).
- [8] Christian Kraglund Andersen, Ants Remm, Stefania Lazar, Sebastian Krinner, Nathan Lacroix, Graham J. Norris, Mihai Gabureac, Christopher Eichler, and Andreas Wallraff. Repeated quantum error detection in a surface code. *Nature Physics*, 16(8): 875–880, Aug 2020. ISSN 1745-2481. DOI: [10.1038/s41567-020-0920-y](https://doi.org/10.1038/s41567-020-0920-y).
- [9] Sebastian Krinner, Nathan Lacroix, Ants Remm, Agustin Di Paolo, Elie Genois, Catherine Leroux, Christoph Hellings, Stefania Lazar, Francois Swiadek, Johannes Herrmann, Graham J. Norris, Christian Kraglund Andersen, Markus Müller, Alexandre Blais, Christopher Eichler, and Andreas Wallraff. Realizing repeated quantum error correction in a distance-three surface code. *Nature*, 605(7911):669–674, May 2022. ISSN 1476-4687. DOI: [10.1038/s41586-022-04566-8](https://doi.org/10.1038/s41586-022-04566-8).
- [10] Luca Pezzé and Augusto Smerzi. Entanglement, nonlinear dynamics, and the heisenberg limit. *Phys. Rev. Lett.*, 102: 100401, Mar 2009. DOI: [10.1103/PhysRevLett.102.100401](https://doi.org/10.1103/PhysRevLett.102.100401).
- [11] Rafał Demkowicz-Dobrzański, Jan Kołodyński, and Mădălin Guţă. The elusive heisenberg limit in quantum-enhanced metrology. *Nature Communications*, 3(11): 1063, Sep 2012. ISSN 2041-1723. DOI: [10.1038/ncomms2067](https://doi.org/10.1038/ncomms2067).
- [12] Sisi Zhou, Mengzhen Zhang, John Preskill, and Liang Jiang. Achieving the heisenberg limit in quantum metrology using quantum error correction. *Nature Communications*, 9 (11):78, Jan 2018. ISSN 2041-1723. DOI: [10.1038/s41467-017-02510-3](https://doi.org/10.1038/s41467-017-02510-3).
- [13] Gui-lu Long, Fu-guo Deng, Chuan Wang, Xi-han Li, Kai Wen, and Wan-ying Wang. Quantum secure direct communication and deterministic secure quantum communication. *Frontiers of Physics in China*, 2(3): 251–272, Jul 2007. ISSN 1673-3606. DOI: [10.1007/s11467-007-0050-3](https://doi.org/10.1007/s11467-007-0050-3).
- [14] Jian-Yong Hu, Bo Yu, Ming-Yong Jing, Lian-Tuan Xiao, Suo-Tang Jia, Guo-Qing Qin, and Gui-Lu Long. Experimental quantum secure direct communication with single photons. *Light: Science & Applications*, 5(99):e16144–e16144, Sep 2016. ISSN 2047-7538. DOI: [10.1038/lsa.2016.144](https://doi.org/10.1038/lsa.2016.144).

- [15] Wei Zhang, Dong-Sheng Ding, Yu-Bo Sheng, Lan Zhou, Bao-Sen Shi, and Guang-Can Guo. Quantum secure direct communication with quantum memory. *Phys. Rev. Lett.*, 118:220501, May 2017. DOI: [10.1103/PhysRevLett.118.220501](https://doi.org/10.1103/PhysRevLett.118.220501).
- [16] Dik Bouwmeester, Jian-Wei Pan, Klaus Mattle, Manfred Eibl, Harald Weinfurter, and Anton Zeilinger. Experimental quantum teleportation. *Nature*, 390(66606660): 575–579, Dec 1997. ISSN 1476-4687. DOI: [10.1038/37539](https://doi.org/10.1038/37539).
- [17] A. Furusawa, J. L. Sørensen, S. L. Braunstein, C. A. Fuchs, H. J. Kimble, and E. S. Polzik. Unconditional quantum teleportation. *Science*, 282(5389):706–709, Oct 1998. DOI: [10.1126/science.282.5389.706](https://doi.org/10.1126/science.282.5389.706).
- [18] M. A. Nielsen, E. Knill, and R. Laflamme. Complete quantum teleportation using nuclear magnetic resonance. *Nature*, 396(67066706):52–55, Nov 1998. ISSN 1476-4687. DOI: [10.1038/23891](https://doi.org/10.1038/23891).
- [19] M. Riebe, H. Häffner, C. F. Roos, W. Hänsel, J. Benhelm, G. P. T. Lancaster, T. W. Körber, C. Becher, F. Schmidt-Kaler, D. F. V. James, and R. Blatt. Deterministic quantum teleportation with atoms. *Nature*, 429(69936993):734–737, Jun 2004. ISSN 1476-4687. DOI: [10.1038/nature02570](https://doi.org/10.1038/nature02570).
- [20] Ph. Nozières and Annie Blandin. Kondo effect in real metals. *Journal de Physique*, 41(3):193–211, 1980. DOI: [10.1051/jphys:01980004103019300](https://doi.org/10.1051/jphys:01980004103019300).
- [21] Jun Kondo. *The Physics of Dilute Magnetic Alloys*. Cambridge University Press, 2012. DOI: [10.1017/CBO9781139162173](https://doi.org/10.1017/CBO9781139162173).
- [22] D. M. Basko, I. L. Aleiner, and B. L. Altshuler. Metal-insulator transition in a weakly interacting many-electron system with localized single-particle states. *Annals of Physics*, 321(5):1126–1205, 2006. ISSN 0003-4916. DOI: [10.1016/j.aop.2005.11.014](https://doi.org/10.1016/j.aop.2005.11.014).
- [23] Rahul Nandkishore and David A. Huse. Many-body localization and thermalization in quantum statistical mechanics. *Annual Review of Condensed Matter Physics*, 6(1):15–38, 2015. DOI: [10.1146/annurev-conmatphys-031214-014726](https://doi.org/10.1146/annurev-conmatphys-031214-014726).
- [24] Horst L. Stormer, Daniel C. Tsui, and Arthur C. Gossard. The fractional quantum hall effect. *Rev. Mod. Phys.*, 71:S298–S305, Mar 1999. DOI: [10.1103/RevModPhys.71.S298](https://doi.org/10.1103/RevModPhys.71.S298).
- [25] Adolfo Avella and Ferdinando Mancini. *Strongly Correlated Systems: Theoretical Methods*. Springer, Berlin Heidelberg, 01 2012. ISBN 978-3-642-21830-9. DOI: [10.1007/978-3-642-21831-6](https://doi.org/10.1007/978-3-642-21831-6).
- [26] Henrik Bruus and Karsten Flensberg. *Many-body quantum theory in condensed matter physics: an introduction*. OUP Oxford, 2004. ISBN 978-0-19-856633-5.
- [27] Iacopo Carusotto and Cristiano Ciuti. Quantum fluids of light. *Rev. Mod. Phys.*, 85: 299–366, Feb 2013. DOI: [10.1103/RevModPhys.85.299](https://doi.org/10.1103/RevModPhys.85.299).
- [28] Immanuel Bloch, Jean Dalibard, and Wilhelm Zwerger. Many-body physics with ultracold gases. *Rev. Mod. Phys.*, 80:885–964, Jul 2008. DOI: [10.1103/RevModPhys.80.885](https://doi.org/10.1103/RevModPhys.80.885).
- [29] Gabriele Campagnano, Oded Zilberberg, Igor V. Gornyi, Dmitri E. Feldman, Andrew C. Potter, and Yuval Gefen. Hanbury brown–twiss interference of anyons. *Phys. Rev. Lett.*, 109:106802, Sep 2012. DOI: [10.1103/PhysRevLett.109.106802](https://doi.org/10.1103/PhysRevLett.109.106802).
- [30] Hassan Shapourian, Ken Shiozaki, and Shinsei Ryu. Partial time-reversal transformation and entanglement negativity in fermionic systems. *Phys. Rev. B*, 95:165101, Apr 2017. DOI: [10.1103/PhysRevB.95.165101](https://doi.org/10.1103/PhysRevB.95.165101).
- [31] T. M. R. Wolf, J. L. Lado, G. Blatter, and O. Zilberberg. Electrically tunable flat bands and magnetism in twisted bilayer graphene. *Phys. Rev. Lett.*, 123:096802, Aug 2019. DOI: [10.1103/PhysRevLett.123.096802](https://doi.org/10.1103/PhysRevLett.123.096802).
- [32] Tobias M. R. Wolf, Oded Zilberberg, Gianni Blatter, and Jose L. Lado. Spontaneous valley spirals in magnetically encapsulated twisted bilayer graphene. *Phys. Rev. Lett.*, 126:056803, Feb 2021. DOI: [10.1103/PhysRevLett.126.056803](https://doi.org/10.1103/PhysRevLett.126.056803).
- [33] J. L. Lado and Oded Zilberberg. Topological spin excitations in harper-heisenberg spin chains. *Phys. Rev. Research*, 1: 033009, Oct 2019. DOI: [10.1103/PhysRevResearch.1.033009](https://doi.org/10.1103/PhysRevResearch.1.033009).
- [34] Antonio Štrkalj, Elmer V. H. Doggen, Igor V. Gornyi, and Oded Zilberberg. Many-body localization in the interpolating aubry-andré-fibonacci model. *Phys. Rev. Research*,

- 3:033257, Sep 2021. DOI: [10.1103/PhysRevResearch.3.033257](https://doi.org/10.1103/PhysRevResearch.3.033257).
- [35] Andisheh Khedri, Antonio Štrkalj, Alessio Chiochetta, and Oded Zilberberg. Luttinger liquid coupled to ohmic-class environments. *Phys. Rev. Research*, 3: L032013, Jul 2021. DOI: [10.1103/PhysRevResearch.3.L032013](https://doi.org/10.1103/PhysRevResearch.3.L032013).
- [36] Michael S. Ferguson, Leon C. Camenzind, Clemens Müller, Daniel E. F. Biesinger, Christian P. Scheller, Bernd Braunecker, Dominik M. Zumbühl, and Oded Zilberberg. Quantum measurement induces a many-body transition. *arXiv:2010.04635 [cond-mat]*, Oct 2020. DOI: [10.48550/ARXIV.2010.04635](https://doi.org/10.48550/ARXIV.2010.04635).
- [37] Michael Sven Ferguson, Oded Zilberberg, and Gianni Blatter. Open quantum systems beyond fermi’s golden rule: Diagrammatic expansion of the steady-state time-convolutionless master equations. *Phys. Rev. Research*, 3:023127, May 2021. DOI: [10.1103/PhysRevResearch.3.023127](https://doi.org/10.1103/PhysRevResearch.3.023127).
- [38] Yaodong Li, Xiao Chen, and Matthew P. A. Fisher. Quantum zeno effect and the many-body entanglement transition. *Phys. Rev. B*, 98:205136, Nov 2018. DOI: [10.1103/PhysRevB.98.205136](https://doi.org/10.1103/PhysRevB.98.205136).
- [39] M. Szyniszewski, A. Romito, and H. Schomerus. Entanglement transition from variable-strength weak measurements. *Phys. Rev. B*, 100:064204, Aug 2019. DOI: [10.1103/PhysRevB.100.064204](https://doi.org/10.1103/PhysRevB.100.064204).
- [40] Yuhan Liu, Ramanjit Sohal, Jonah Kudler-Flam, and Shinsei Ryu. Multipartitioning topological phases by vertex states and quantum entanglement. *Phys. Rev. B*, 105: 115107, Mar 2022. DOI: [10.1103/PhysRevB.105.115107](https://doi.org/10.1103/PhysRevB.105.115107).
- [41] Mohan Sarovar, Akihito Ishizaki, Graham R. Fleming, and K. Birgitta Whaley. Quantum entanglement in photosynthetic light-harvesting complexes. *Nature Physics*, 6(66): 462–467, Jun 2010. ISSN 1745-2481. DOI: [10.1038/nphys1652](https://doi.org/10.1038/nphys1652).
- [42] Filippo Caruso, Alex W. Chin, Animesh Datta, Susana F. Huelga, and Martin B. Plenio. Entanglement and entangling power of the dynamics in light-harvesting complexes. *Phys. Rev. A*, 81:062346, Jun 2010. DOI: [10.1103/PhysRevA.81.062346](https://doi.org/10.1103/PhysRevA.81.062346).
- [43] Akihito Ishizaki and Graham R Fleming. Quantum superpositions in photosynthetic light harvesting: delocalization and entanglement. *New Journal of Physics*, 12(5): 055004, may 2010. DOI: [10.1088/1367-2630/12/5/055004](https://doi.org/10.1088/1367-2630/12/5/055004).
- [44] Evert van Nieuwenburg and Oded Zilberberg. Entanglement spectrum of mixed states. *Phys. Rev. A*, 98:012327, Jul 2018. DOI: [10.1103/PhysRevA.98.012327](https://doi.org/10.1103/PhysRevA.98.012327).
- [45] Lidia Stocker, Stefan H. Sack, Michael S. Ferguson, and Oded Zilberberg. Entanglement-based observables for quantum impurities. *Phys. Rev. Res.*, 4:043177, Dec 2022. DOI: [10.1103/PhysRevResearch.4.043177](https://doi.org/10.1103/PhysRevResearch.4.043177).
- [46] D. Perez-Garcia, F. Verstraete, M. M. Wolf, and J. I. Cirac. Matrix product state representations. *arXiv:quant-ph/0608197*, May 2007. DOI: [10.48550/ARXIV.QUANT-PH/0608197](https://doi.org/10.48550/ARXIV.QUANT-PH/0608197).
- [47] U. Schollwöck. The density-matrix renormalization group. *Rev. Mod. Phys.*, 77: 259–315, Apr 2005. DOI: [10.1103/RevModPhys.77.259](https://doi.org/10.1103/RevModPhys.77.259).
- [48] Ulrich Schollwöck. The density-matrix renormalization group in the age of matrix product states. *Annals of Physics*, 326(1): 96–192, Jan 2011. ISSN 00034916. DOI: [10.1016/j.aop.2010.09.012](https://doi.org/10.1016/j.aop.2010.09.012).
- [49] Rajibul Islam, Ruichao Ma, Philipp M. Preiss, M. Eric Tai, Alexander Lukin, Matthew Rispoli, and Markus Greiner. Measuring entanglement entropy in a quantum many-body system. *Nature*, 528(75807580): 77–83, Dec 2015. ISSN 1476-4687. DOI: [10.1038/nature15750](https://doi.org/10.1038/nature15750).
- [50] Leonid Gurvits. Classical deterministic complexity of edmonds’ problem and quantum entanglement. *arXiv:quant-ph/0303055*, Mar 2003. DOI: [10.48550/arXiv.quant-ph/0303055](https://doi.org/10.48550/arXiv.quant-ph/0303055).
- [51] Sevag Gharibian. Strong np-hardness of the quantum separability problem. *arXiv:0810.4507 [quant-ph]*, Dec 2009. DOI: [10.48550/ARXIV.0810.4507](https://doi.org/10.48550/ARXIV.0810.4507).
- [52] G. Vidal and R. F. Werner. Computable measure of entanglement. *Phys. Rev. A*, 65:032314, Feb 2002. DOI: [10.1103/PhysRevA.65.032314](https://doi.org/10.1103/PhysRevA.65.032314).
- [53] Pasquale Calabrese, John Cardy, and Erik

- Tonni. Entanglement negativity in quantum field theory. *Phys. Rev. Lett.*, 109:130502, Sep 2012. DOI: [10.1103/PhysRevLett.109.130502](https://doi.org/10.1103/PhysRevLett.109.130502).
- [54] Pasquale Calabrese, John Cardy, and Erik Tonni. Entanglement negativity in extended systems: a field theoretical approach. *Journal of Statistical Mechanics: Theory and Experiment*, 2013(02):P02008, Feb 2013. ISSN 1742-5468. DOI: [10.1088/1742-5468/2013/02/P02008](https://doi.org/10.1088/1742-5468/2013/02/P02008).
- [55] Elisabeth Wybo, Michael Knap, and Frank Pollmann. Entanglement dynamics of a many-body localized system coupled to a bath. *Phys. Rev. B*, 102:064304, Aug 2020. DOI: [10.1103/PhysRevB.102.064304](https://doi.org/10.1103/PhysRevB.102.064304).
- [56] Shengqi Sang, Yaodong Li, Tianci Zhou, Xiao Chen, Timothy H. Hsieh, and Matthew P. A. Fisher. Entanglement negativity at measurement-induced criticality. *PRX Quantum*, 2:030313, Jul 2021. DOI: [10.1103/PRXQuantum.2.030313](https://doi.org/10.1103/PRXQuantum.2.030313).
- [57] Matthias Christandl and Andreas Winter. “squashed entanglement”: An additive entanglement measure. *Journal of Mathematical Physics*, 45(3):829–840, 2004. DOI: [10.1063/1.1643788](https://doi.org/10.1063/1.1643788).
- [58] Souvik Dutta and Thomas Faulkner. A canonical purification for the entanglement wedge cross-section. *Journal of High Energy Physics*, 2021(3):178, Mar 2021. ISSN 1029-8479. DOI: [10.1007/JHEP03\(2021\)178](https://doi.org/10.1007/JHEP03(2021)178).
- [59] Zhanyu Ma, Cheolhee Han, Yigal Meir, and Eran Sela. Symmetric inseparability and number entanglement in charge-conserving mixed states. *Phys. Rev. A*, 105:042416, Apr 2022. DOI: [10.1103/PhysRevA.105.042416](https://doi.org/10.1103/PhysRevA.105.042416).
- [60] Paolo Zanardi. Entanglement of quantum evolutions. *Phys. Rev. A*, 63:040304(R), Mar 2001. DOI: [10.1103/PhysRevA.63.040304](https://doi.org/10.1103/PhysRevA.63.040304).
- [61] Tomaž Prosen and Iztok Pižorn. Operator space entanglement entropy in a transverse ising chain. *Phys. Rev. A*, 76:032316, Sep 2007. DOI: [10.1103/PhysRevA.76.032316](https://doi.org/10.1103/PhysRevA.76.032316).
- [62] Iztok Pižorn and Tomaž Prosen. Operator space entanglement entropy in xy spin chains. *Phys. Rev. B*, 79:184416, May 2009. DOI: [10.1103/PhysRevB.79.184416](https://doi.org/10.1103/PhysRevB.79.184416).
- [63] Hui Li and F. D. M. Haldane. Entanglement spectrum as a generalization of entanglement entropy: Identification of topological order in non-abelian fractional quantum hall effect states. *Phys. Rev. Lett.*, 101:010504, Jul 2008. DOI: [10.1103/PhysRevLett.101.010504](https://doi.org/10.1103/PhysRevLett.101.010504).
- [64] J Dubail. Entanglement scaling of operators: a conformal field theory approach, with a glimpse of simulability of long-time dynamics in $1 + 1d$. *Journal of Physics A: Mathematical and Theoretical*, 50(23):234001, may 2017. DOI: [10.1088/1751-8121/aa6f38](https://doi.org/10.1088/1751-8121/aa6f38).
- [65] Evert P. L. van Nieuwenburg and Sebastian D. Huber. Classification of mixed-state topology in one dimension. *Phys. Rev. B*, 90:075141, Aug 2014. DOI: [10.1103/PhysRevB.90.075141](https://doi.org/10.1103/PhysRevB.90.075141).
- [66] Eyal Cornfeld, Moshe Goldstein, and Eran Sela. Imbalance entanglement: Symmetry decomposition of negativity. *Phys. Rev. A*, 98:032302, Sep 2018. DOI: [10.1103/PhysRevA.98.032302](https://doi.org/10.1103/PhysRevA.98.032302).
- [67] Katarzyna Macieszczak, Emanuele Levi, Tommaso Macrì, Igor Lesanovsky, and Juan P. Garrahan. Coherence, entanglement, and quantumness in closed and open systems with conserved charge, with an application to many-body localization. *Phys. Rev. A*, 99:052354, May 2019. DOI: [10.1103/PhysRevA.99.052354](https://doi.org/10.1103/PhysRevA.99.052354).
- [68] Ryszard Horodecki, Paweł Horodecki, Michał Horodecki, and Karol Horodecki. Quantum entanglement. *Rev. Mod. Phys.*, 81:865–942, Jun 2009. DOI: [10.1103/RevModPhys.81.865](https://doi.org/10.1103/RevModPhys.81.865).
- [69] Gilad Gour, Markus P. Müller, Varun Narasimhachar, Robert W. Spekkens, and Nicole Yunger Halpern. The resource theory of informational nonequilibrium in thermodynamics. *Physics Reports*, 583:1–58, 2015. ISSN 0370-1573. DOI: <https://doi.org/10.1016/j.physrep.2015.04.003>.
- [70] Alexander Streltsov, Hermann Kampermann, Sabine Wölk, Manuel Gessner, and Dagmar Bruß. Maximal coherence and the resource theory of purity. *New Journal of Physics*, 20(5):053058, may 2018. DOI: [10.1088/1367-2630/aac484](https://doi.org/10.1088/1367-2630/aac484).
- [71] Daniel Manzano. A short introduction to the lindblad master equation. *AIP Advances*, 10(2):025106, Feb 2020. DOI: [10.1063/1.5115323](https://doi.org/10.1063/1.5115323).
- [72] F. Verstraete, J. J. García-Ripoll, and J. I.

- Cirac. Matrix product density operators: Simulation of finite-temperature and dissipative systems. *Phys. Rev. Lett.*, 93:207204, Nov 2004. DOI: [10.1103/PhysRevLett.93.207204](https://doi.org/10.1103/PhysRevLett.93.207204).
- [73] Matthew Fishman, Steven R. White, and E. Miles Stoudenmire. The itensor software library for tensor network calculations. *SciPost Phys. Codebases*, page 4, 2022. DOI: [10.21468/SciPostPhysCodeb.4](https://doi.org/10.21468/SciPostPhysCodeb.4).
- [74] Adil A. Gangat, Te I, and Ying-Jer Kao. Steady states of infinite-size dissipative quantum chains via imaginary time evolution. *Phys. Rev. Lett.*, 119:010501, Jul 2017. DOI: [10.1103/PhysRevLett.119.010501](https://doi.org/10.1103/PhysRevLett.119.010501).
- [75] Mark H Fischer, Mykola Maksymenko, and Ehud Altman. Dynamics of a many-body-localized system coupled to a bath. *Phys. Rev. Lett.*, 116:160401, Apr 2016. DOI: [10.1103/PhysRevLett.116.160401](https://doi.org/10.1103/PhysRevLett.116.160401).
- [76] EPL van Nieuwenburg, J Yago Malo, AJ Daley, and MH Fischer. Dynamics of many-body localization in the presence of particle loss. *Quantum Science and Technology*, 3(1):01LT02, dec 2017. DOI: [10.1088/2058-9565/aa9a02](https://doi.org/10.1088/2058-9565/aa9a02).
- [77] Zala Lenarčič, Ori Alberton, Achim Rosch, and Ehud Altman. Critical behavior near the many-body localization transition in driven open systems. *Phys. Rev. Lett.*, 125:116601, Sep 2020. DOI: [10.1103/PhysRevLett.125.116601](https://doi.org/10.1103/PhysRevLett.125.116601).
- [78] Christopher David White, Michael Zaletel, Roger S. K. Mong, and Gil Refael. Quantum dynamics of thermalizing systems. *Phys. Rev. B*, 97:035127, Jan 2018. DOI: [10.1103/PhysRevB.97.035127](https://doi.org/10.1103/PhysRevB.97.035127).
- [79] Daniel Jaschke, Simone Montangero, and Lincoln D Carr. One-dimensional many-body entangled open quantum systems with tensor network methods. *Quantum Science and Technology*, 4(1):013001, nov 2018. DOI: [10.1088/2058-9565/aac724](https://doi.org/10.1088/2058-9565/aac724).
- [80] Maxime Dupont, Nicholas E. Sherman, and Joel E. Moore. Spatiotemporal crossover between low- and high-temperature dynamical regimes in the quantum heisenberg magnet. *Phys. Rev. Lett.*, 127:107201, Aug 2021. DOI: [10.1103/PhysRevLett.127.107201](https://doi.org/10.1103/PhysRevLett.127.107201).
- [81] Alessio Lerose, Michael Sonner, and Dmitry A. Abanin. Influence matrix approach to many-body floquet dynamics. *Phys. Rev. X*, 11:021040, May 2021. DOI: [10.1103/PhysRevX.11.021040](https://doi.org/10.1103/PhysRevX.11.021040).
- [82] Michael Sonner, Alessio Lerose, and Dmitry A. Abanin. Influence functional of many-body systems: Temporal entanglement and matrix-product state representation. *Annals of Physics*, 435:168677, 2021. ISSN 0003-4916. DOI: <https://doi.org/10.1016/j.aop.2021.168677>.
- [83] Alexander Lukin, Matthew Rispoli, Robert Schittko, M. Eric Tai, Adam M. Kaufman, Soonwon Choi, Vedika Khemani, Julian Léonard, and Markus Greiner. Probing entanglement in a many-body-localized system. *Science*, 364(6437):256–260, 2019. DOI: [10.1126/science.aau0818](https://doi.org/10.1126/science.aau0818).
- [84] Tiff Brydges, Andreas Elben, Petar Jurcevic, Benoît Vermersch, Christine Maier, Ben P. Lanyon, Peter Zoller, Rainer Blatt, and Christian F. Roos. Probing rényi entanglement entropy via randomized measurements. *Science*, 364(6437):260–263, 2019. DOI: [10.1126/science.aau4963](https://doi.org/10.1126/science.aau4963).
- [85] John Preskill. Quantum Computing in the NISQ era and beyond. *Quantum*, 2:79, August 2018. ISSN 2521-327X. DOI: [10.22331/q-2018-08-06-79](https://doi.org/10.22331/q-2018-08-06-79).
- [86] Michael Brooks. Beyond quantum supremacy: the hunt for useful quantum computers. *Nature*, 574(7776):19–21, Oct 2019. DOI: [10.1038/d41586-019-02936-3](https://doi.org/10.1038/d41586-019-02936-3).
- [87] Eric Carlen. Trace inequalities and quantum entropy: an introductory course. *Contemp. Math.*, 529:73–140, 2010. DOI: [10.1090/conm/529/10428](https://doi.org/10.1090/conm/529/10428).
- [88] Chandler Davis. A schwarz inequality for convex operator functions. *Proceedings of the American Mathematical Society*, 8(1):42–44, 1957. ISSN 00029939, 10886826. DOI: <https://doi.org/10.2307/2032808>.

A Properties of the configuration coherence

In the main text, we introduce the configuration coherence in terms of the density matrix (2) and the \mathcal{C} -matrix (4) as

$$C_N(\rho) := \sum_{n \neq n'} \text{Tr}(\mathcal{C}_{n,n'}) = \sum_{n \neq n'} \sum_{\substack{i_n, j_{n'} \\ \mu_n, \nu_{n'}}} |\rho_{i_n, \mu_n; j_{n'}, \nu_{n'}}|^2. \quad (16)$$

Here, we prove the properties 1, 2, 3, and 4 of the configuration coherence introduced in the main text. To this end, we provide two alternative definitions of the configuration coherence in terms of local particle number projectors. As in the main text, we will assume that the system has a fixed particle number N , but the discussion is valid for any fixed charge.

We define the local projectors Π_n^B that measure the particle number in subsystem B . The completeness relation of the projectors is $\sum_n \Pi_n^B = \mathbb{1}^B$ and they are orthogonal, $\Pi_n^B \Pi_m^B = \delta_{nm} \Pi_n^B$. These projectors allow for an alternative formulation of the configuration coherence:

Proposition A.1. *The configuration coherence is given as*

$$C_N(\rho) = \sum_{n \neq n'} \|(\mathbb{1}^A \otimes \Pi_n^B) \rho (\mathbb{1}^A \otimes \Pi_{n'}^B)\|^2, \quad (17)$$

where $\|A\| = \sqrt{\text{Tr}(A^\dagger A)}$ is the Frobenius norm.

Proof. Using the particle number basis $|i_n, \mu_n\rangle = |i_n\rangle_A \otimes |\mu_n\rangle_B$, we can write $\Pi_n^B = \sum_{\mu_n} |\mu_n\rangle\langle\mu_n|$. Expressing the density matrix in the same basis, we find

$$\begin{aligned} \rho_{n,n'} &:= (\mathbb{1}^A \otimes \Pi_n^B) \rho (\mathbb{1}^A \otimes \Pi_{n'}^B) \\ &= (\mathbb{1}^A \otimes \sum_{\mu_n} |\mu_n\rangle\langle\mu_n|) \left[\sum_{m,m'} \sum_{\substack{i_m, \mu_m \\ j_{m'}, \nu_{m'}}} \rho_{i_m, \mu_m; j_{m'}, \nu_{m'}} |i_m, \mu_m\rangle\langle j_{m'}, \nu_{m'}| \right] (\mathbb{1}^A \otimes \sum_{\mu_{n'}} |\mu_{n'}\rangle\langle\mu_{n'}|) \\ &= \sum_{\substack{i_n, \mu_n \\ j_{n'}, \nu_{n'}}} \rho_{i_n, \mu_n; j_{n'}, \nu_{n'}} |i_n, \mu_n\rangle\langle j_{n'}, \nu_{n'}|. \end{aligned} \quad (18)$$

Next, we calculate the Frobenius norm squared of this matrix as

$$\|\rho_{n,n'}\|^2 = \text{Tr}(\rho_{n,n'}^\dagger \rho_{n,n'}) = \sum_{\substack{i_n, \mu_n \\ j_{n'}, \nu_{n'}}} |\rho_{i_n, \mu_n; j_{n'}, \nu_{n'}}|^2 = \text{Tr}(\mathcal{C}_{n,n'}). \quad (19)$$

Finally, we find

$$C_N(\rho) = \sum_{n \neq n'} \text{Tr}(\mathcal{C}_{n,n'}) = \sum_{n \neq n'} \|\rho_{n,n'}\|^2 = \sum_{n \neq n'} \|(\mathbb{1}^A \otimes \Pi_n^B) \rho (\mathbb{1}^A \otimes \Pi_{n'}^B)\|^2. \quad (20)$$

□

Proposition A.2. *The configuration coherence is given as*

$$C_N(\rho) = \text{Tr}\left((\rho - \rho_\Pi)^2\right), \quad (21)$$

with the locally measured density matrix

$$\rho_\Pi := \sum_n (\mathbb{1}^A \otimes \Pi_n^B) \rho (\mathbb{1}^A \otimes \Pi_n^B). \quad (22)$$

Proof. Due to orthogonality of the local projectors, it holds that $\|\rho_{n,n'} + \rho_{m,m'}\|^2 = \|\rho_{n,n'}\|^2 + \|\rho_{m,m'}\|^2$ for $(n, n') \neq (m, m')$. By inserting two identities $\mathbb{1} = \sum_n \mathbb{1}^A \otimes \Pi_n^B$, we find

$$\begin{aligned} \text{Tr}((\rho - \rho_\Pi)^2) &= \|\rho - \rho_\Pi\|^2 = \|\mathbb{1}\rho\mathbb{1} - \rho_\Pi\|^2 = \left\| \sum_{n,n'} (\mathbb{1}^A \otimes \Pi_n^B) \rho (\mathbb{1}^A \otimes \Pi_{n'}^B) - \sum_n (\mathbb{1}^A \otimes \Pi_n^B) \rho (\mathbb{1}^A \otimes \Pi_n^B) \right\|^2 \\ &= \left\| \sum_{n \neq n'} (\mathbb{1}^A \otimes \Pi_n^B) \rho (\mathbb{1}^A \otimes \Pi_{n'}^B) \right\|^2 = \left\| \sum_{n \neq n'} \rho_{n,n'} \right\|^2 = \sum_{n \neq n'} \|\rho_{n,n'}\|^2 = C_N(\rho). \end{aligned} \quad (23)$$

□

Note that the form (21) shows the close relation of the configuration coherence with the number entanglement, which is the relative entropy between ρ and ρ_Π [59]. This means that both measures are sensitive to the same flavour of quantum correlations, namely the one between different sub-charge sectors.

Proposition A.3. *The configuration coherence is convex, i.e.,*

$$\sum_i p_i C_N(\rho_i) \geq C_N\left(\sum_i p_i \rho_i\right), \quad (24)$$

for density matrices ρ_i and $\sum_i p_i = 1$.

Proof. First we prove that

$$\lambda C_N(\rho) + (1 - \lambda) C_N(\sigma) \geq C_N(\lambda \rho + (1 - \lambda) \sigma), \quad (25)$$

with density matrices ρ, σ and $0 \leq \lambda \leq 1$. The measurement $\rho \mapsto \rho_\Pi$ is linear, thus

$$\begin{aligned} C_N(\lambda \rho + (1 - \lambda) \sigma) &= \text{Tr}(\lambda(\rho - \rho_\Pi) + (1 - \lambda)(\sigma - \sigma_\Pi))^2 \\ &\leq \lambda \text{Tr}((\rho - \rho_\Pi))^2 + (1 - \lambda) \text{Tr}((\sigma - \sigma_\Pi))^2 = \lambda C_N(\rho) + (1 - \lambda) C_N(\sigma), \end{aligned} \quad (26)$$

where the inequality follows from the convexity conservation of the trace function [87] and the convexity of $f(t) = t^2$.

Next, we repeatedly use statement (25) and find

$$\begin{aligned} C_N\left(\sum_i p_i \rho_i\right) &= C_N\left(p_1 \rho_1 + (1 - p_1) \underbrace{\sum_{i>1} \frac{p_i}{1 - p_1} \rho_i}_{\sigma_1}\right) \leq p_1 C_N(\rho_1) + (1 - p_1) C_N(\sigma_1) \\ &= p_1 C_N(\rho_1) + (1 - p_1) C_N\left(\frac{p_2}{1 - p_1} \rho_2 + \frac{1 - p_1 - p_2}{1 - p_1} \underbrace{\sum_{i>2} \frac{p_i}{1 - p_1 - p_2} \rho_i}_{\sigma_2}\right) \\ &\leq p_1 C_N(\rho_1) + p_2 C_N(\rho_2) + (1 - p_1 - p_2) C_N(\sigma_2) \leq \dots \leq \sum_i p_i C_N(\rho_i). \end{aligned} \quad (27)$$

The $\sigma_j = \sum_{i>j} \frac{p_i}{1 - \sum_{k \leq j} p_k} \rho_i$ define valid density matrices because

$$\frac{1}{1 - \sum_{k \leq j} p_k} \sum_{i>j} p_i \underbrace{\quad}_{\sum_i p_i = 1} = \frac{1}{1 - \sum_{k \leq j} p_k} \left(1 - \sum_{k \leq j} p_k\right) = 1. \quad (28)$$

□

Proposition A.4. *The configuration coherence vanishes for separable states $\rho_{\text{sep}} = \sum_i p_i \rho_i^A \otimes \rho_i^B$ with fixed particle number.*

Proof. Due to the convexity property A.3, it suffices to show that the configuration coherence vanishes for a product state $\rho = \rho^A \otimes \rho^B$. We use the total particle number operator

$$\hat{N} = \hat{N}^A \otimes \mathbb{1}^B + \mathbb{1}^A \otimes \hat{N}^B, \quad (29)$$

with the local particle number operators $\hat{N}^{A,B} = \sum_n n \Pi_n^{A,B}$. Due to the fixed particle number, it holds that $[\rho, \hat{N}] = 0$. Using the partial trace Tr_A over subsystem A , we find

$$\begin{aligned} 0 &= \text{Tr}_A([\rho, \hat{N}]) = \text{Tr}_A([\rho^A \otimes \rho^B, \hat{N}^A \otimes \mathbb{1}^B + \mathbb{1}^A \otimes \hat{N}^B]) \\ &= \text{Tr}(\rho^A \hat{N}^A) \rho^B + \underbrace{\text{Tr}(\rho^A)}_{=1} (\rho^B \hat{N}^B) - \underbrace{\text{Tr}(\hat{N}^A \rho^A)}_{=\text{Tr}(\rho^A \hat{N}^A)} \rho^B - \underbrace{\text{Tr}(\rho^A)}_{=1} (\hat{N}^B \rho^B) \\ &= \rho^B \hat{N}^B - \hat{N}^B \rho^B = [\rho^B, \hat{N}^B] = \sum_n n [\rho^B, \Pi_n^B]. \end{aligned} \quad (30)$$

Due to the orthogonality of the projectors, it follows $[\rho^B, \Pi_n^B] = 0, \forall n$. Thus, for a product state, the locally measured density matrix (22) is equivalent to the density matrix, $(\rho^A \otimes \rho^B)_\Pi = \rho^A \otimes \rho^B$. From the form (21) it follows that the configuration coherence must vanish for a product state, and therefore for separable states. \square

Proposition A.5. *The configuration coherence is invariant under local particle number conserving unitary operations.*

Proof. Let $U = U^A \otimes U^B$ be a local unitary transformation, i.e., $UU^\dagger = U^\dagger U = \mathbb{1}$. The particle number conservation translates to $[U, \hat{N}] = 0$. By replacing $\rho \mapsto U$ in (30) and noting that $\text{Tr}_A U^A \neq 0$, we find $[U, \mathbb{1}^A \otimes \Pi_n^B] = 0 \forall n$. From the latter, it follows for the locally measured density matrix (22) that $U \rho_\Pi U^\dagger = (U \rho U^\dagger)_\Pi$. Thus,

$$\begin{aligned} C_N(U \rho U^\dagger) &= \text{Tr} \left(\left(U \rho U^\dagger - (U \rho U^\dagger)_\Pi \right)^2 \right) = \text{Tr} \left(\left(U \rho U^\dagger - U \rho_\Pi U^\dagger \right)^2 \right) \\ &= \text{Tr} \left(\left(U (\rho - \rho_\Pi) U^\dagger \right)^2 \right) = \text{Tr} \left((\rho - \rho_\Pi)^2 \right) = C_N(\rho), \end{aligned} \quad (31)$$

where the second-to-last equality follows from the unitarity of U and the cyclic property of the trace. \square

Proposition A.6. *The configuration coherence is monotonous under local purity non-increasing particle number conserving operations.*

Proof. We consider a local charge conserving operation $\rho \mapsto \mathcal{E}(\rho) = \sum_i K_i \rho K_i^\dagger$, with Kraus operators $K_i = K_i^A \otimes K_i^B$ satisfying $\sum_i K_i^\dagger K_i = \mathbb{1}$. The particle number conservation implies $[K_i, \mathbb{1}^A \otimes \Pi_n^B] = 0$ (proof is equivalent to proof of $[U, \mathbb{1}^A \otimes \Pi_n^B] = 0$ for A.5). The most general purity non-increasing maps are unital maps [69, 70], i.e., $\sum_i K_i K_i^\dagger = \mathbb{1}$. Using the fact that $\|\rho_{n,n'} + \rho_{m,m'}\|^2 = \|\rho_{n,n'}\|^2 + \|\rho_{m,m'}\|^2$ for $(n, n') \neq (m, m')$, we rewrite the configuration coherence (16) as

$$C_N(\rho) = \sum_{n' \neq n} \|\rho_{n,n'}\|^2 = \sum_{n' > n} \|\rho_{n,n'}\|^2 + \|\rho_{n',n}\|^2 = \sum_{n' > n} \|\rho_{n,n'} + \rho_{n',n}\|^2 = \sum_{n' > n} \text{Tr}(\rho_{n,n'} + \rho_{n',n})^2. \quad (32)$$

Note that the matrices $\rho_{n,n'} + \rho_{n',n}$ are Hermitian.

We prove the monotonicity in two steps. First, we show that $\mathcal{E}(\rho)_{n,n'} + \mathcal{E}(\rho)_{n',n} = \mathcal{E}(\rho_{n,n'} + \rho_{n',n})$. Secondly, we prove that $\|\mathcal{E}(\rho_{n,n'} + \rho_{n',n})\|^2 \leq \|\rho_{n,n'} + \rho_{n',n}\|^2 \forall n' > n$ using Jensen's trace inequality.

For the first step, we have

$$\begin{aligned}\mathcal{E}(\rho)_{n,n'} &= (\mathbb{1}^A \otimes \Pi_n^B) \mathcal{E}(\rho) (\mathbb{1}^A \otimes \Pi_{n'}^B) = (\mathbb{1}^A \otimes \Pi_n^B) \sum_i K_i \rho K_i^\dagger (\mathbb{1}^A \otimes \Pi_{n'}^B) \\ &\stackrel{[K_i, \mathbb{1}^A \otimes \Pi_n^B]=0}{=} \sum_i K_i (\mathbb{1}^A \otimes \Pi_n^B) \rho (\mathbb{1}^A \otimes \Pi_{n'}^B) K_i^\dagger = \mathcal{E}(\rho_{n,n'}) ,\end{aligned}\quad (33)$$

From the linearity of \mathcal{E} , it follows that

$$\mathcal{E}(\rho)_{n,n'} + \mathcal{E}(\rho)_{n',n} = \mathcal{E}(\rho_{n,n'}) + \mathcal{E}(\rho_{n',n}) = \mathcal{E}(\rho_{n,n'} + \rho_{n',n}) . \quad (34)$$

For the second step, we use Jensen's trace inequality [88], which states that

$$\mathrm{Tr} \left(f \left(\sum_i K_i X_i K_i^\dagger \right) \right) \leq \mathrm{Tr} \left(\sum_i K_i f(X_i) K_i^\dagger \right) , \quad (35)$$

for convex f , Hermitian matrices X_i and quadratic K_i satisfying $\sum_i K_i K_i^\dagger = \mathbb{1}$. From setting $X_i = \rho_{n,n'} + \rho_{n',n} \forall i$ and using the unitality of \mathcal{E} and the convexity of $f(t) = t^2$, it follows that

$$\begin{aligned}\mathrm{Tr}(\mathcal{E}(\rho)_{n,n'} + \mathcal{E}(\rho)_{n',n})^2 &= \mathrm{Tr}(\mathcal{E}(\rho_{n,n'} + \rho_{n',n}))^2 = \mathrm{Tr} \left(\sum_i K_i (\rho_{n,n'} + \rho_{n',n}) K_i^\dagger \right)^2 \\ &\stackrel{\text{Jensen}}{\leq} \mathrm{Tr} \left(\sum_i K_i (\rho_{n,n'} + \rho_{n',n})^2 K_i^\dagger \right) = \mathrm{Tr} \left((\rho_{n,n'} + \rho_{n',n})^2 \underbrace{\sum_i K_i^\dagger K_i}_{=\mathbb{1}} \right) \\ &= \mathrm{Tr}(\rho_{n,n'} + \rho_{n',n})^2 .\end{aligned}\quad (36)$$

Finally, we find that

$$C_N(\mathcal{E}(\rho)) = \sum_{n' > n} \mathrm{Tr}(\mathcal{E}(\rho)_{n,n'} + \mathcal{E}(\rho)_{n',n})^2 \leq \sum_{n' > n} \mathrm{Tr}(\rho_{n,n'} + \rho_{n',n})^2 = C_N(\rho) \quad (37)$$

Note that for general quantum maps, the K_i do not have to be quadratic, and in that case Jensen's trace inequality does not apply. However, we are interested in situations where the system's Hilbert space is fixed, which requires that the map \mathcal{E} is built from quadratic Kraus operators K_i . \square

B Rank of the \mathcal{C} -matrix

In the main text, we introduce the \mathcal{C} -matrix (4) whose eigenvalues define the operator-space entanglement spectrum (OSSES). For fixed particle number, the matrix has a block diagonal structure [cf. eq. (9) and Fig. 1(d)]. Here, we discuss the rank of these blocks in more detail.

In a matrix product density operator (MPDO) representation of the mixed state density matrix [72], the rank of the \mathcal{C} -matrix defines the necessary bond dimension χ_{exact} of the MPDO to represent the state exactly. We can calculate the rank by summing over the ranks of the individual blocks of the \mathcal{C} -matrix.

The blocks are given by

$$\mathcal{C}_{n,n'} = \sum_{i_n, j_{n'}, k_n, l_{n'}} c_{i_n, j_{n'}; k_n, l_{n'}} |i_n, j_{n'}\rangle \langle\langle k_n, l_{n'}| , \quad (38)$$

with coefficients

$$c_{i_n, j_{n'}; k_n, l_{n'}} = \sum_{\mu_n, \nu_{n'}} \rho_{i_n, \mu_n; j_{n'}, \nu_{n'}} \rho_{k_n, \mu_n; l_{n'}, \nu_{n'}}^* . \quad (39)$$

Reordering the summation, we can write the block (38) as

$$\mathcal{C}_{n,n'} = \sum_{\mu_n, \nu_{n'}} v_{\mu_n, \nu_{n'}} v_{\mu_n, \nu_{n'}}^\dagger, \quad (40)$$

with vectors

$$v_{\mu_n, \nu_{n'}} = \sum_{i_n, j_{n'}} \rho_{i_n, \mu_n; j_{n'}, \nu_{n'}} |i_n, j_{n'}\rangle. \quad (41)$$

The length of the vector (41) and thus the size of the block (38) is determined by the number of possible supervectors $|i_n, j_{n'}\rangle$.

If we denote the size of subsystem A by L_A , then there are $\binom{L_A}{n}$ possible states $|i_n\rangle$ of n particles in subsystem A . It follows that the size of the block (38) is given by $\binom{L_A}{n} \times \binom{L_A}{n'}$. At the same time, the form (40) reveals that the block $\mathcal{C}_{n,n'}$ is a sum over rank-1 matrices $v_{\mu_n, \nu_{n'}} v_{\mu_n, \nu_{n'}}^\dagger$. Consequently, there are $\binom{L_B}{N-n} \times \binom{L_B}{N-n'}$ of these matrices, with L_B the size of subsystem B . As the rank of a matrix sum is bounded by the sum of the ranks of the summands, we find that the block $\mathcal{C}_{n,n'}$ has a maximal rank

$$\text{rank} \mathcal{C}_{n,n'} = \min \left(\binom{L_A}{n} \times \binom{L_A}{n'}, \binom{L_B}{N-n} \times \binom{L_B}{N-n'} \right), \quad (42)$$

with L_A (L_B) the size of subsystem A (B). It follows that the maximal bond dimension for N particles is given by

$$\chi_{\text{exact}} = \sum_{n,n'=0}^N \min \left(\binom{L_A}{n} \times \binom{L_A}{n'}, \binom{L_B}{N-n} \times \binom{L_B}{N-n'} \right). \quad (43)$$

The maximal rank (43) for N particles in a system of size L scales as $\chi_{\text{exact}} \propto L^N$ (stemming from the blocks with $n + n' = N$). Thus, if the number of particles is fixed, the maximal rank has a power-law scaling with system size, as opposed to the exponential scaling in the general setting. This permits simulation of very large system sizes with fixed particle number. Table 1 shows the maximal ranks per block for the example of $N = 2$ particles. As expected, the maximal bond dimension scales as L^2 .

block	(n, n')	degeneracy	maximal rank
AA	(2, 2)	1	1
AC	(2, 1)	2	$\frac{L}{2}$
AB	(1, 1)	1	$\left(\frac{L}{2}\right)^2$
BC	(0, 1)	2	$\frac{L}{2}$
BB	(0, 0)	1	1
CC	(2, 0)	2	$\frac{L}{4} \left(\frac{L}{2} - 1\right)$
maximal bond dimension			$\frac{L^2}{2} + \frac{3L}{2} + 2$

Table 1: Maximal ranks of the blocks of the \mathcal{C} -matrix for $N = 2$ particles on a chain of length L and bipartition in the middle. The maximal bond dimension is obtained as the sum over the maximal ranks times the corresponding degeneracies.

Several factors can reduce the maximal bond dimension (43). In particular, under the assumption of local decoherence, cf. Ref. [44], the blocks $\mathcal{C}_{N,0}$ and $\mathcal{C}_{0,N}$ become rank 1.

C Configuration coherence and negativity for a single particle

In this section, we show the equivalence of the configuration coherence (12) to the negativity for a mixed state of a single particle. Recall that the negativity is given as the sum over the negative eigenvalues of the partially transposed density matrix [52].

We use the particle number basis $|i_n, \mu_n\rangle = |i_n\rangle_A \otimes |\mu_n\rangle_B$ and that for a single particle, it holds $n \in [0, 1]$. Therefore, we can define $|i\rangle_A := |i_1\rangle_A$ and $|\mu\rangle_B := |\mu_1\rangle_B$. Note that the only state with zero particles in a subsystem is the vacuum state $|0\rangle_{A,B}$. With this, the density matrix (2) for a single particle can be written as

$$\begin{aligned} \rho = & \left(\sum_{i,j \in A} \rho_{i,0;j,0} |i\rangle\langle j|_A \right) \otimes |0\rangle\langle 0|_B + |0\rangle\langle 0|_A \otimes \left(\sum_{\mu,\nu \in B} \rho_{0,\mu;0,\nu} |\mu\rangle\langle \nu|_B \right) \\ & + \sum_{i \in A, \mu \in B} \rho_{i,0;0,\mu} |i\rangle_A |0\rangle_B \langle 0|_A \langle \mu|_B + \rho_{0,\mu;i,0} |0\rangle_A |\mu\rangle_B \langle i|_A \langle 0|_B. \end{aligned} \quad (44)$$

The partial transpose of (44) has a block-diagonal form, and only one block has a negative eigenvalue. It is the block describing the particle in a coherent cross-boundary state,

$$\rho_C^{T_A} = \sum_{i \in A, \mu \in B} \rho_{i,0;0,\mu} |0\rangle_A |0\rangle_B \langle i|_A \langle \mu|_B + \rho_{i,0;0,\mu}^* |i\rangle_A |\mu\rangle_B \langle 0|_A \langle 0|_B = |0\rangle\langle \phi|_{AB} + |\phi\rangle\langle 0|_{AB}, \quad (45)$$

with the non normalized vector

$$|\phi\rangle_{AB} := \sum_{i \in A, \mu \in B} \rho_{i,0;0,\mu}^* |i\rangle_A |\mu\rangle_B. \quad (46)$$

A rank-2 block of the form (45) has two eigenvalues $\pm \sqrt{\langle 0|0\rangle_{AB} \langle \phi|\phi\rangle_{AB}} = \pm \sqrt{\langle \phi|\phi\rangle_{AB}}$. Thus, the negativity for the single particle state (44) is given by

$$\mathcal{N}(\rho) = \sqrt{\langle \phi|\phi\rangle_{AB}} = \sqrt{\sum_{i \in A, \mu \in B} |\rho_{i,0;0,\mu}|^2}. \quad (47)$$

For the configuration coherence (12) of the single particle state (44), we find

$$C_N(\rho) = \text{Tr}(\mathcal{C}_{0,1}) + \text{Tr}(\mathcal{C}_{1,0}) = 2 \times \text{Tr}(\mathcal{C}_{0,1}) = 2 \sum_{i \in A, \mu \in B} |\rho_{i,0;0,\mu}|^2 = 2\mathcal{N}(\rho)^2. \quad (48)$$

Therefore, for mixed states of a single particle, the configuration coherence equals twice the negativity squared.